Nonlinear free vibration analysis of Timoshenko nanobeams with surface energy

ARTICLE *in* MECCANICA · JUNE 2014

Impact Factor: 1.95 · DOI: 10.1007/s11012-014-9992-z

2 AUTHORS:

Reza Nazemnezhad
Damghan University
30 PUBLICATIONS **181** CITATIONS
SEE PROFILE

Shahrokh Hosseini-Hashemi
Iran University of Science and Technol…
94 PUBLICATIONS **1,035** CITATIONS
SEE PROFILE

Meccanica
DOI 10.1007/s11012-014-9992-z

Nonlinear free vibration analysis of Timoshenko nanobeams with surface energy

Reza Nazemnezhad · Shahrokh Hosseini-Hashemi

Received: 24 October 2013 / Accepted: 16 June 2014

Abstract In this study, influences of balance condition and surface density in addition to the surface elasticity and stress on the nonlinear free vibration of Timoshenko and Euler–Bernoulli nanobeams are investigated. In order to consider the balance condition between the nanobeam bulk and its surfaces, it is assumed that the normal stress varies linearly along the nanobeam thickness. Accordingly, the surface density in addition to the surface stress and elasticity is introduced into the governing equations. Moreover, besides using the bulk density, the surface density is also employed to obtain the kinetic energy of the nanobeams. The multiple scale method is used to obtain an analytical solution for the nonlinear governing equations. This results in the modal response frequencies (the amplitude dependence of the response frequencies due to the nonlinearity) of nanobeams. It is observed that considering the surface density effect and satisfying the balance condition cause a reduction in the frequency ratios, and this reduction is a little more for Timoshenko nanobeams than Euler–Bernoulli ones for all types of boundary conditions used. It is believed that this work is a comprehensive study for investigating effects of all components of the surface energy on the linear and nonlinear free vibrations of Timoshenko and Euler–Bernoulli nanobeams with different boundary conditions while the balance condition is also satisfied.

Keywords Nonlinear free vibration · Timoshenko nanobeam · Surface density · Analytical solution · Balance condition

1 Introduction

Owing to their high surface to volume ratio, nanoscale structures exhibit superior mechanical, electrical and thermal performances than their micro- and/or macro-scale counterparts. In micro/nano electromechanical systems (MEMS/NEMS), they are widely used in many areas, including communications, machinery, information technology, biotechnology and etc. [1, 2]. An important phenomenon that has attracted considerable attention in the literature is the size-dependent mechanical behavior of nanobeams due to the surface energy.

R. Nazemnezhad (✉) · S. Hosseini-Hashemi
School of Mechanical Engineering, Iran University of Science and Technology, Narmak, 16842-13114 Tehran, Iran
e-mail: rnazemnezhad@iust.ac.ir; rnazemnezhad@du.ac.ir

R. Nazemnezhad
School of Engineering, Damghan University, Damghan, Iran

S. Hosseini-Hashemi
Center of Excellence in Railway Transportation, Iran University of Science and Technology, Narmak, 16842-13114 Tehran, Iran

Published online: 27 August 2014

In classical continuum mechanics, the surface energy effects are ignored as they are small compared to the bulk energy. For nanoscale materials and structures, however, the surface energy becomes significant due to the high surface to volume ratio. Both the atomistic simulations and experimental evaluations strongly suggest that the ratio of surface to volume plays a critical role in nano-sized problems. To account for the effect of surfaces/interfaces on mechanical deformation, the surface elasticity theory is presented by modeling the surface as a two dimensional membrane adhering to the underlying bulk material without slipping [3, 4]. In order to analyze a nanostructure based on the surface elasticity theory, the balance condition between the nanobeam bulk and its surfaces is suggested to be satisfied [5–7]. In this theory, the energy stored in the surfaces is due to the surface elasticity, the surface stress and the surface density. The surface elasticity theory is used to analyze the nanostructures for different purposes. It can be mentioned to the works done on mechanical properties of nanostructures in the presence of the surface energy [8–15], wave propagation [16–19], Pull-in instability [20, 21], buckling [22–24], post-buckling [25], free vibration [26–32], and electromechanical coupling [33–42]. Most of the papers using the surface elasticity theory only considered the surface stress and elasticity. There are a few papers that all components of the surface energy are considered and the balance condition is satisfied [5–7, 43–46]. For example, Liu and Rajapakse [43] studied the linear static and dynamic behaviors of Timoshenko and Euler–Bernoulli nanobeams when effects of all the components of the surface energy as well as the balance condition are considered simultaneously. They presented a set of closed-form analytical solutions for the linear static response of thin and thick beams under different loading and boundary conditions, as well as the solution of linear free vibration characteristic of such beams. It was shown that natural frequencies and deflections of nanobeams were significantly influenced by the surface energy effect. But, they did not consider effects of the surface elasticity and stress as well as the surface density and the balance condition, separately.

For small oscillations the response of a deformable body can be adequately described by linear equations and boundary conditions. However as the amplitude of oscillation increases, nonlinear effects come into play. The geometric nonlinearity which is caused by nonlinear stretching is one of these nonlinearity effects. Nonlinear stretching of the midplane of a deformable body accompanies its transverse vibrations if it is supported in such a way as to restrict movement of its ends and/or edges. This stretching leads to a nonlinear relationship between the strain and the displacement. This nonlinear relationship causes that on one hand the superposition principle does not be valid for the system, and on the other hand the strain energy of the system be dependent on the amplitude of deflection. Thus, because the natural frequencies depend on the strain energy, they will also be dependent on the amplitude of deflection. In other words, the nonlinear natural frequencies (the modal response frequencies) of systems are amplitude dependence [47–49]. Beside the geometric nonlinearity, nonlinearities coming from slack and electrostatic forces may affect the static and dynamic behaviors of nanostructures [50–52]. The surface elasticity theory of Gurtin–Murdoch is also used for nonlinear analysis of nanostructures [44–46, 53–59]. Gheshlaghi and Hasheminejad [53] studied the nonlinear flexural vibrations of micro- and nanobeams in the presence of the surface elasticity and stress within the framework of Euler–Bernoulli beam theory including the von Kármán geometric nonlinearity. They used Jacobi elliptic functions to obtain the natural frequencies. In another similar work, Malekzadeh and Shojaee [54] investigated the nonlinear free vibration of non-uniform Timoshenko and Euler–Bernoulli nanobeams incorporating only the surface elasticity and stress using the nonlocal elasticity theory. In the work, the differential quadrature method (DQM) was used to obtain the nonlinear vibration frequencies. Nonlinear free vibration analyses of functionally graded Euler–Bernoulli nanobeams can be found in Refs. [56, 57]. Like linear analysis of nanobeams, for the nonlinear analysis of nanobeams there is no work focusing on the influences of the surface density and satisfying the balance condition on the mechanical behavior of them. Whereas for an accurate design and manufacturing of MEMS/NEMS, it is necessary to investigate influences of all effective parameters like the surface density and the balance condition in addition to the surface elasticity and stress effects.

The main goal of the present study is investigating the influences of the surface density and balance condition on the nonlinear free vibrations of

Timoshenko and Euler–Bernoulli nanobeams with three different end conditions, i.e. Simply supported–Simply supported (SS), Simply supported–Clamped (SC) and Clamped–Clamped (CC). To this end, the governing equations including the von kármán geometric nonlinearity are obtained. The nonlinear governing equations are solved analytically using the method of multiple scales. Lastly, the nonlinear free vibration frequencies of nanobeams are presented for various lengths, thickness ratios and amplitude ratios. It is believed that this work is a comprehensive study for investigating all components of the surface energy on linear and nonlinear free vibrations of Timoshenko and Euler–Bernoulli nanobeams with different boundary conditions while the balance condition between the nanobeam bulk and its surfaces is considered to be satisfied.

2 Problem formulation

2.1 Surface elasticity theory

Due to the increasing surface to bulk ratio in nano-sized structures, surface energy is likely to be significant and can considerably modify macroscopic properties. For isotropic surfaces $S^{\pm}$ (S^{+} and S^{-} are the upper and lower surfaces respectively), the following surface constitutive equations are proposed by Gurtin and Murdoch [3, 60]

$$\begin{cases} \tau_{\alpha\beta}^{\pm} = \tau_0^{\pm}\delta_{\alpha\beta} + \left(\mu_0^{\pm} - \tau_0^{\pm}\right)\left(u_{\alpha,\beta}^{\pm} + u_{\beta,\alpha}^{\pm}\right) \\ \quad + \left(\lambda_0^{\pm} + \tau_0^{\pm}\right)u_{\gamma,\gamma}^{\pm}\delta_{\alpha\beta} + \tau_0^{\pm}u_{\alpha,\beta}^{\pm}; \\ \tau_{\alpha z}^{\pm} = \tau_0^{\pm}u_{z,\alpha}^{\pm} \end{cases} \tag{1}$$

where $\tau_{\alpha\beta}^{\pm}$ are the surface stresses, $u_{\alpha,\beta}^{\pm}$ are the surface strains, $\tau_0^{\pm}$ are residual surface tensions under unconstrained conditions, $\mu_0^{\pm}$ and $\lambda_0^{\pm}$ are the surface Lamé constants, $\delta_{\alpha\beta}$ the Kronecker delta, $u_{\alpha}^{\pm}$ are displacement components of the surfaces $S^{\pm}$. In Eq. (1), α and $\beta = x, y$.

2.2 Governing equation for Timoshenko nanobeam

Consider a nanobeam with length L ($0 \le x \le L$), thickness $2h$ ($-h \le z \le h$), and width b ($-b/2 \le y \le +b/2$) (see Fig. 1). Upon using the Timoshenko

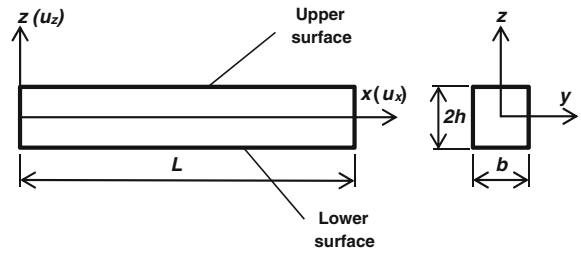

Fig. 1 Geometry of the nanobeam

beam model, the displacement field at any point of the nanobeam can be written as

$$\begin{cases} u_x(x,z,t) = U(x,t) + z\,\psi(x,t) \\ u_z(x,z,t) = W(x,t) \end{cases} \tag{2}$$

where $u_x(x,z,t)$ and $u_z(x,z,t)$ are the displacement fields at any point of the nanobeam along x and z directions, respectively, $U(x,t)$ and $W(x,t)$ are the displacement components of the mid-plane at time t, and $\psi(x,t)$ is the rotation of beam cross section. The von kármán type nonlinear strain–displacement relationship is given by

$$\varepsilon_{xx} = \frac{\partial u_x}{\partial x} + \frac{1}{2}\left(\frac{\partial u_z}{\partial x}\right)^2 = \frac{\partial U}{\partial x} + z\frac{\partial \psi}{\partial x} + \frac{1}{2}\left(\frac{\partial W}{\partial x}\right)^2 \tag{3}$$

$$\gamma_{xz} = \frac{\partial W}{\partial x} + \psi \tag{4}$$

where ε_{xx} and γ_{xz} are the axial and shear strains, respectively.

Assuming a homogeneous isotropic material and neglecting any residual stress in the bulk due to surface stress, the simplified constitutive stress–strain relations of the nanobeam bulk can be written as

$$\sigma_{xx} = E\,\varepsilon_{xx} + \upsilon\,\sigma_{zz} \tag{5}$$

$$\tau_{xx} = kG\left(\psi + \frac{\partial W}{\partial x}\right) \tag{6}$$

where σ_{zz} is the bulk stress component along the nanobeam thickness, ε_{xx} is the strain along the nanobeam length, τ_{xx} is the shear stress, E is Young's modulus, υ is Poisson's ratio, k is the shear correction factor and G is shear modulus.

Assuming the same material properties for the top and the bottom layers of the nanobeam, the stress–strain relations, i.e. Eq. (1), for the Timoshenko nanobeam model reduce to

$$\begin{cases} \tau_{xx} = \tau_0 + E^s \varepsilon_{xx} \\ \tau_{xz} = \tau_0 \dfrac{\partial w}{\partial x} \end{cases} \tag{7}$$

where $E^s = 2\mu_0 + \lambda_0$ is the surface elasticity.

The stress components of the surface layers must satisfy the following equilibrium relations [3, 60]

$$\begin{cases} \tau^+_{\beta i,\beta} - \sigma^+_{iz} = \rho_{\prime} \dfrac{\partial^2 u_i^+}{\partial t^2} \quad at \quad z = +h \\ \tau^-_{\beta i,\beta} + \sigma^-_{iz} = \rho_0 \dfrac{\partial^2 u_i^-}{\partial t^2} \quad at \quad z = -h \end{cases} \tag{8}$$

where the surface stresses of the nanobeam are denoted by $\tau^+_{\beta i}$ and $\tau^-_{\beta i}$. $\sigma^+_{iz} = \sigma_{iz}$ $(z = +h)$ and $\sigma^-_{iz} = \sigma_{iz}$ $(z = -h)$ are bulk stresses. ρ_0 is the surface density of surface layers. In Eq. (8), $\beta = x, y$ and $i = x, y, z$.

By substituting Eqs. (2) and (7) into Eq. (8), the following equations can be obtained

$$\begin{cases} \sigma^+_{zz} = \tau_0 \dfrac{\partial^2 w}{\partial x^2} - \rho_0 \dfrac{\partial^2 w}{\partial t^2} \\ \sigma^-_{zz} = -\tau_0 \dfrac{\partial^2 w}{\partial x^2} + \rho_0 \dfrac{\partial^2 w}{\partial t^2} \end{cases} \tag{9}$$

In the classical Timoshenko beam theory, the bulk stress component, σ_{zz}, is assumed to be zero. However, the surface equilibrium equations of Gurtin–Murdoch [3, 60] model will not be satisfied with this assumption. Therefore, it is assumed that the bulk stress component, σ_{zz}, varies linearly through the nanobeam thickness [7]. Therefore it can be expressed as

$$\sigma_{zz} = \frac{1}{2}\left(\sigma^+_{zz} + \sigma^-_{zz}\right) + \frac{z}{2h}\left(\sigma^+_{zz} - \sigma^-_{zz}\right) \tag{10}$$

Substitution of Eq. (9) into Eq. (10) gives

$$\sigma_{zz} = \frac{z}{h}\left(\tau_0 \frac{\partial^2 w}{\partial x^2} - \rho_0 \frac{\partial^2 w}{\partial t^2}\right) \tag{11}$$

The effect of the residual surface stress on the beam is specified by the Laplace–Young equation [4, 61]. It gives the distributed loading on the two surfaces as follows

$$\begin{cases} p_1(x) = \tau^+_{\beta i} b \dfrac{\partial^2 u_z}{\partial x^2} \\ p_2(x) = \tau^-_{\beta i} b \dfrac{\partial^2 u_z}{\partial x^2} \end{cases} \tag{12}$$

Therefore, the superposition of two residual surface tensions can be implemented by an effective transverse distributed loading along the nanobeam longitudinal direction, $p(x)$, in the following form

$$p(x) = 2\tau_0 b \frac{\partial^2 w}{\partial x^2} \tag{13}$$

Now, by using Hamilton's principle, the nonlinear equations of motion of the Timoshenko nanobeam can be derived as

$$\frac{\partial N_{xx}}{\partial x} = m \frac{\partial^2 U}{\partial t^2} \tag{14}$$

$$\frac{\partial}{\partial x}\left(N_{xx} \frac{\partial W}{\partial x}\right) + \frac{\partial Q_{xz}}{\partial x} + 2b\tau_0 \frac{\partial^2 W}{\partial x^2} = m \frac{\partial^2 W}{\partial t^2} \tag{15}$$

$$\frac{\partial \mathrm{M_{xx}}}{\partial_{\mathrm{x}}} - \mathrm{Q_{xz}} = (\rho\, \mathrm{I})^* \frac{\partial^2 \psi}{\partial \mathrm{t}^2} \tag{16}$$

where $m = \rho A + 2b\rho_0$ and $(\rho I)^* = \rho I + \rho_0(2bh^2 + 4h^3/3)$. By setting the surface energy terms equal zero, the nonlinear equations of motion of the conventional Timoshenko beam [62] will be obtained from Eqs. (14–16). N_{xx}, M_{xx} and Q_{xz} are also the local force resultant, bending moment resultant and transverse shear force, respectively, and given by

$$\begin{aligned} N_{xx} &= \int \sigma_{xx} dA + 2\int \sigma^s_{xx} dz + \int \sigma^s_{xx} dy\big|_{z=+h} \\ &\quad + \int \sigma^s_{xx} dy\big|_{z=-h} = (EA + E^s(4h + 2b))\left(\frac{\partial U}{\partial x}\right) \\ &\quad + \left(\frac{EA}{2} + E^s(2h + b)\right)\left(\frac{\partial W}{\partial x}\right)^2 \end{aligned} \tag{17}$$

$$\begin{aligned} M_{xx} &= \int \sigma_{xx} z dA + 2\int \sigma^s_{xx} z dz + \int \sigma^s_{xx}(+h) dy\big|_{z=+h} \\ &\quad + \int \sigma^s_{xx}(-h) dy\big|_{z=-h} = \left(EA + E^s\left(\frac{4h^3}{3} + 2bh^2\right)\right) \\ &\quad \left(\frac{\partial \psi}{\partial x}\right) + \frac{\tau_0 \upsilon I}{h}\frac{\partial^2 W}{\partial x^2} - \frac{\rho_0 \upsilon I}{h}\frac{\partial^2 W}{\partial t^2} \end{aligned} \tag{18}$$

$$Q_{xz} = \int_A \tau_{xz} dA = kAG\left(\psi + \frac{\partial W}{\partial x}\right) \tag{19}$$

If the axial inertia is neglected, Eq. (14) gives

$$\frac{\partial^2 U}{\partial t^2} = 0 \Rightarrow \frac{\partial N_{xx}}{\partial x} = 0 \Rightarrow N_{xx} = N_0 = Constant \tag{20}$$

With Eq. (20) in mind and for Timoshenko nanobeams with immovable ends (i.e. U and $W = 0$,

at $x = 0$ and L), integrating Eq. (17) with respect to x leads to

$$N_{xx} = N_0 = \left(\frac{EA + 2E^s(2h+b)}{2L}\right)\int_0^L \left(\frac{\partial W}{\partial x}\right)^2 dx \tag{21}$$

Now, substituting Eqs. (18) and (19) in Eqs. (15) and (16) and using Eq. (21) lead to the nonlinear governing equations for the Timoshenko nanobeam with the surface energy as follow

$$N_{xx}\frac{\partial^2 W}{\partial x^2} + kAG\left(\frac{\partial \psi}{\partial x} + \frac{\partial^2 W}{\partial x^2}\right) + 2b\tau_0\frac{\partial^2 W}{\partial x^2} = m\frac{\partial^2 W}{\partial t^2} \tag{22}$$

$$\begin{aligned}&\left[EI + E^s\left(\frac{4h^3}{3} + 2bh^2\right)\right]\frac{\partial^2 \psi}{\partial x^2} + \frac{\tau_0 \upsilon I}{h}\frac{\partial^3 W}{\partial x^3}\\ &-\frac{\rho_0 \upsilon I}{h}\frac{\partial^3 W}{\partial x \partial t^2} - kAG\left(\psi + \frac{\partial W}{\partial x}\right)\\ &= (\rho I)^*\frac{\partial^2 \psi}{\partial t^2}\end{aligned} \tag{23}$$

In order to decouple Eqs. (22) and (23), rewriting Eq. (22) results in

$$\frac{\partial \psi}{\partial x} = -\frac{N_{xx}}{kAG}\frac{\partial^2 W}{\partial x^2} - \frac{\partial^2 W}{\partial x^2} - \frac{2b\tau_0}{kAG}\frac{\partial^2 W}{\partial x^2} + \frac{m}{kAG}\frac{\partial^2 W}{\partial t^2} \tag{24}$$

Differentiation Eq. (23) respect to x also gives

$$\begin{aligned}&\left[EI + E^s\left(\frac{4h^3}{3} + 2bh^2\right)\right]\frac{\partial^2}{\partial x^2}\left(\frac{\partial \psi}{\partial x}\right) + \frac{\tau_0 \upsilon I}{h}\frac{\partial^4 W}{\partial x^4}\\ &-\frac{\rho_0 \upsilon I}{h}\frac{\partial^4 W}{\partial x^2 \partial t^2} - kAG\left(\left(\frac{\partial \psi}{\partial x}\right) + \frac{\partial^2 W}{\partial x^2}\right)\\ &= (\rho I)^*\frac{\partial^2}{\partial t^2}\left(\frac{\partial \psi}{\partial x}\right)\end{aligned} \tag{25}$$

Finally, substituting Eq. (24) into Eq. (25) decouples Eqs. (22) and (23), and the following equation that governs the transverse deflection W will be obtained

$$\begin{aligned}&(EI)_{eff}\frac{\partial^4 W}{\partial x^4} + (\rho I)_{eff}\frac{\partial^4 W}{\partial x^2 \partial t^2} - (2b\tau_0)\frac{\partial^2 W}{\partial x^2}\\ &+\left((\rho I)^*\frac{m}{kAG}\right)\frac{\partial^4 W}{\partial t^4} + (m)\frac{\partial^2 W}{\partial t^2}\\ &+N_0\left[-\frac{\partial^2 W}{\partial x^2} - \left(\frac{(\rho I)^*}{kAG}\right)\frac{\partial^4 W}{\partial x^2 \partial t^2} + (EI)^{nl}_{eff}\frac{\partial^4 W}{\partial x^4}\right] = 0\end{aligned} \tag{26}$$

in which

$$\begin{aligned}(EI)_{eff} &= \left(EI + E^s\left(4h^3/3 + 2bh^2\right)\right)(2b\tau_0/kAG + 1)\\ &\quad - \tau_0 \upsilon I/h;\\ (\rho I)_{eff} &= -\left(\left(EI + E^s\left(4h^3/3 + 2bh^2\right)\right)(m/kAG)\right.\\ &\quad \left.+(\rho I)^*(2b\tau_0/kAG + 1) - \rho_0 \upsilon I/h\right);\\ (EI)^{nl}_{eff} &= \left(EI + E^s\left(4h^3/3 + 2bh^2\right)\right)/kAG\end{aligned}$$

The equation of motion of the conventional nonlinear Timoshenko beam theory [62] can be obtained from Eq. (26) by setting $E^s = \tau_0 = \rho_0 = 0$.

3 Nonlinear free vibration analysis

For free vibration analysis, it is convenient to work with dimensionless quantities, since such a formulation will facilitate the identification of the order of magnitude of some variables. Hence let

$$\hat{t} = \omega t; \quad \hat{x} = x/L; \quad \hat{W} = W/L \tag{27}$$

where $\omega = (n\pi/L)^2(EI/\rho A)^{0.5}$ is the linear frequency for a simply supported Euler–Bernoulli nanobeam without considering the surface energy and the balance condition effects. Substitution of Eq. (27) into Eq. (26) and use of the chain rule of differentiation will make Eq. (26) in nondimensional form as

$$\begin{aligned}&\left(\frac{(EI)_{eff}}{L^3}\right)\frac{\partial^4 W}{\partial x^4} + \left(\frac{\omega^2(\rho I)_{eff}}{L}\right)\frac{\partial^4 W}{\partial x^2 \partial t^2}\\ &-\left(\frac{(2b\tau_0)}{L}\right)\frac{\partial^2 W}{\partial x^2} + (L\omega^4)\left((\rho I)^*\frac{m}{kAG}\right)\frac{\partial^4 W}{\partial t^4}\\ &+(m)(L\omega^2)\frac{\partial^2 W}{\partial t^2} + \bar{N}_0\left[\left(\frac{-1}{L}\right)\frac{\partial^2 W}{\partial x^2}\right.\\ &\left.-\left(\frac{\omega^2}{L}\right)\left(\frac{(\rho I)^*}{kAG}\right)\frac{\partial^4 W}{\partial x^2 \partial t^2} + \left(\frac{(EI)^{nl}_{eff}}{L^3}\right)\frac{\partial^4 W}{\partial x^4}\right] = 0\end{aligned} \tag{28}$$

where

$$\begin{aligned}\bar{N}_0 &= 0.5(EA + 2E^s(2h+b))\\ &\int_0^1 \left(\frac{\partial W}{\partial x}\right)^2 dx = P\int_0^1 \left(\frac{\partial W}{\partial x}\right)^2 dx\\ P &= 0.5(EA + 2E^s(2h+b))\end{aligned}$$

(In the above and hereinafter we drop the caret on all the quantities and variables for notational convenience).

For nonlinear free vibration analysis, the single mode and multimode Galerkin's method can be used to convert Eq. (28) to an ordinary differential equation [63, 64]. At low amplitude ratios, the effect of the number of modes has a minor effect on the nonlinear frequency ratios of nanobeams [65]. Thus, the single mode Galerkin's method can provide the nonlinear natural frequency of nanobeams with good accuracy. As the amplitude ratio increases, the effect of coupling of modes increases [66]. Therefore, the multimode Galerkin's method should be used for nonlinear vibration analysis of nanobeams. In the present study, the single mode Galerkin's method is used. Hence the transverse displacement of the nth mode can be assumed to be

$$W(x,t) = \phi(x) \cdot q(t) \tag{29}$$

where $q(t)$ is a time dependent function to be determined and $\phi(x)$ is the linear mode shape given by

- *Simply supported–simply supported:*

$$\phi_{SS}(x) = Sin(S_1 x) - \frac{Sin(S_1)}{Sinh(S_2)}\mathrm{Sinh}(S_2 x);$$

- *Simply supported–Clamped:*

$$\phi_{SC}(x) = Sin(\zeta_1 x) - \frac{Sin(\zeta_1)}{Sinh(\zeta_2)}\mathrm{Sinh}(\zeta_2 x);$$

- *Clamped–Clamped*

$$\begin{aligned}\phi_{CC}(x) = {} & Sin(\zeta_1 x) - \left(\frac{K_a}{K_b}\right)\mathrm{Sinh}(\zeta_2 x) \\ & + \left(K_a \frac{Cos(\zeta_1) - \mathrm{Cosh}(\zeta_2)}{K_a Sin(\zeta_1) + K_b Sinh(\zeta_2)}\right)(Cos(\zeta_1 x) \\ & - \mathrm{Cosh}(\zeta_2 x));\end{aligned} \tag{30}$$

where parameters $S_{1,2}$ and $\zeta_{1,2}$ can be determined from the eigenvalue equations

- *Simply supported–simply supported:*

$$Sin(S_1)Sinh(S_2) = 0 \tag{31}$$

- *Simply supported–Clamped:*

$$K_b \cdot Tan(\zeta_1) - K_a \cdot Tanh(\zeta_2) = 0$$

- *Clamped–Clamped*

$$\begin{aligned}& 2K_a K_b(1 - Cos(\zeta_1) \cdot Cosh(\zeta_2)) \\ & \quad + \left(K_b^2 - K_a^2\right)Sin(\zeta_1) \cdot Sinh(\zeta_2) = 0\end{aligned}$$

The parameters $S_{1,2}$, $\zeta_{1,2}$, K_a and K_b are given in "Appendix". Substituting Eq. (29) and its derivatives into Eq. (28), then multiplying by the linear mode shape and integrating along the length of nanobeam, results in

$$\ddot{q} + \left(\alpha_1 + \alpha_2 q^2\right)\ddot{q} + \alpha_3 q + \alpha_4 q^3 = 0 \tag{32}$$

where the dot signifies the derivative with respect to time and the coefficients α_i are given by

$$\alpha_1 = \left((\rho I)^* \beta_1 + (L\omega^2)(m)\beta_4\right)/\lambda\beta_4 \tag{33}$$

$$\alpha_2 = -P\beta_3\beta_1/(L\omega^2)(\rho A)L\beta_4 \tag{34}$$

$$\alpha_3 = \left((EI)^* \beta_2 + H\beta_1\right)/\lambda\beta_4 \tag{35}$$

$$\alpha_4 = P\beta_3(L\eta\beta_2 - \beta_1)/L\lambda\beta_4 \tag{36}$$

The coefficients β_i, $(EI)^*$, $(\rho I)^{**}$, H, λ and η are given by

$$\begin{aligned}& \beta_1 = \int_0^1 \left(\phi \cdot \frac{d^2\phi}{dx^2}\right)dx; \quad \beta_2 = \int_0^1 \left(\phi \cdot \frac{d^4\phi}{dx^4}\right)dx; \\ & \beta_3 = \int_0^1 \left(\frac{d\phi}{dx}\right)^2 dx; \quad \beta_4 = \int_0^1 \left(\phi^2\right)dx; \\ & (EI)^* = \frac{(EI)_{eff}}{L^3}; \quad (\rho I)^{**} = \frac{(\rho I)_{eff}\omega^2}{L}; \\ & H = -\frac{2b\tau_0}{L}; \quad \lambda = \frac{\rho I \rho A L \omega^4}{kAG}; \quad \eta = \frac{(EI)^{nl}_{eff}}{L^3};\end{aligned} \tag{37}$$

Since Eq. (32) is fourth-order, one needs to specify four initial conditions. Hence, one lets

$$q(0) = W_{\max}/L; \quad \dot{q}(0) = \ddot{q}(0) = \dddot{q}(0) = 0 \tag{38}$$

where W_{max} is the central amplitude for n = odd.

3.1 Application of the method of multiple scales

For seeking an analytical solution to Eq. (32), the method of multiple scales has been used [67]. In using the multiple scale method, one seeks a second-order

uniform expansion of the solution of Eq. (32) in the form

$$q(t) = \sum_{j=1}^{3} \varepsilon^j q_j(T_0, T_1, T_2) + \cdots \tag{39}$$

where ε is a small parameter that measures the amplitude of oscillation. It is used as a book-keeping device and set equal to unity if the amplitude is taken to be small. One defines a fast time scale $T_0 = t$, on which the main oscillatory behavior occurs, and slow time scales $T_j = \varepsilon^j t$, $j \geq 1$, on which amplitude and phase modulation takes place. The operation of time differentiation is thus expanded as

$$\frac{d}{dt} = D_0 + \varepsilon D_1 + \varepsilon^2 D_2 + \cdots \tag{40}$$

$$\frac{d^2}{dt^2} = D_0^2 + 2\varepsilon D_0 D_1 + \varepsilon^2 \left(D_1^2 + 2D_0 D_2\right) + \cdots \tag{41}$$

$$\frac{d^4}{dt^4} = D_0^4 + 4\varepsilon D_0^3 D_1 + \varepsilon^2 \left(6D_0^2 D_1^2 + 4D_0^3 D_2\right) + \cdots \tag{42}$$

where $D_j = \partial/\partial T_j$.

One then substitutes Eqs. (39) and (37)–(39) into Eq. (32) and equates the like powers of ε to zero to obtain the following hierarchy of linear differential equations which are to be solved successively. These equations are

$$D_0^4 q_1 + \alpha_1 D_0^2 q_1 + \alpha_3 q_1 = 0 \tag{43}$$

$$D_0^4 q_2 + \alpha_1 D_0^2 q_2 + \alpha_3 q_2 = -4D_0^3 D_1 q_1 - 2\alpha_1 D_0 D_1 q_1 \tag{44}$$

$$\begin{aligned} D_0^4 q_3 + \alpha_1 D_0^2 q_3 + \alpha_3 q_3 = &-\left(6D_0^2 D_1^2 + 4D_0^3 D_2\right) q_1 \\ &- \alpha_1 \left(D_1^2 + 2D_0 D_2\right) q_1 \\ &- \alpha_2 q_1^2 D_0^2 q_1 - 4D_0^3 D_1 q_2 - 2\alpha_1 D_0 D_1 q_2 - \alpha_4 q_1^3 \end{aligned} \tag{45}$$

The general solution of Eq. (40) is expressed in the following complex form

$$\begin{aligned} q_1(T_0, T_1, T_2) = &A_1(T_1, T_2) e^{i\omega_1 T_0} \\ &+ A_2(T_1, T_2) e^{i\omega_2 T_0} + cc \end{aligned} \tag{46}$$

where $A_{1,2}$ are unknown complex functions and cc stands for the complex conjugate of the preceding terms. $\omega_{1,2}$ are the linear frequencies given by

$$\omega_{1,2}^2 = \frac{\alpha_1}{2} \mp \sqrt{\frac{\alpha_1^2}{4} - \alpha_3} \tag{47}$$

Equation (44) indicates that for a Timoshenko-type nanobeam there are two bands of linear frequencies denoted by the subscripts 1 (bending modes) and 2 (shear modes), respectively. Substituting Eq. (43) into Eq. (41) leads to

$$\begin{aligned} D_0^4 q_2 + \alpha_1 D_0^2 q_2 + \alpha_3 q_2 = &2i\omega_1 \left(2\omega_1^2 - \alpha_1\right) D_1 A_1 e^{i\omega_1 T_0} \\ &+ 2i\omega_2 \left(2\omega_2^2 - \alpha_1\right) D_1 A_2 e^{i\omega_2 T_0} + cc \end{aligned} \tag{48}$$

The right-hand side of Eq. (45) is resonant and one requires it vanish in order to avoid secular behavior in q_2. This is accomplished by setting $D_1 A_1 = 0$ and $D_1 A_2 = 0$. Therefore A_1 and A_2 must be independent of T_1 or equivalently $A_1 = A_1(T_2)$ and $A_2 = A_2(T_2)$. With $D_1 A_1 = 0$ and $D_1 A_2 = 0$, the solution of Eq. (45) is $q_2 = 0$, in which the solution of the homogeneous equation is not needed [67].

Substituting of Eq. (43) into Eq. (42) and recalling that $q_2 = 0$, $D_1 A_1 = 0$ and $D_1 A_2 = 0$, it can be obtained

$$\begin{aligned} D_0^4 q_3 + \alpha_1 D_0^2 q_3 + \alpha_3 q_3 = &\left\{2i\omega_1 \left(2\omega_1^2 - \alpha_1\right) D_2 A_1 \right. \\ &+ 3\left(\alpha_2 \omega_1^2 - \alpha_4\right) A_1^2 \bar{A}_1 \\ &\left. + 2\left[\alpha_2 \left(\omega_1^2 + 2\omega_2^2\right) - 3\alpha_4\right] A_1 A_2 \bar{A}_2 \right\} e^{i\omega_1 T_0} \\ &+ \left\{2i\omega_2 \left(2\omega_2^2 - \alpha_1\right) D_2 A_2 + 3\left(\alpha_2 \omega_2^2 - \alpha_4\right) A_2^2 \bar{A}_2 \right. \\ &\left. + 2\left[\alpha_2 \left(\omega_2^2 + 2\omega_1^2\right) - 3\alpha_4\right] A_1 \bar{A}_1 A_2 \right\} e^{i\omega_2 T_0} \\ &+ \left[\alpha_2 \left(\omega_1^2 + 2\omega_2^2\right) - 3\alpha_4\right] \left\{A_1 A_2^2 e^{i(\omega_1 + 2\omega_2) T_0} \right. \\ &\left. + A_1 \bar{A}_2^2 e^{i(\omega_1 - 2\omega_2) T_0} \right\} + \left[\alpha_2 \left(\omega_2^2 + 2\omega_1^2\right) - 3\alpha_4\right] \\ &\left\{A_1^2 A_2 e^{i(2\omega_1 + \omega_2) T_0} + A_1^2 \bar{A}_2 e^{i(2\omega_1 - \omega_2) T_0} \right\} \\ &+ \left\{\left[\alpha_2 \omega_1^2 - \alpha_4\right] A_1^3 e^{3i\omega_1 T_0} + \left[\alpha_2 \omega_2^2 - \alpha_4\right] A_2^3 e^{3i\omega_2 T_0} \right\} \\ &+ cc \end{aligned} \tag{49}$$

Eliminating secular terms from q_3 requires that

$$\begin{aligned} &2i\omega_1 \left(2\omega_1^2 - \alpha_1\right) D_2 A_1 + 3\left(\alpha_2 \omega_1^2 - \alpha_4\right) A_1^2 \bar{A}_1 \\ &\quad + 2\left[\alpha_2 \left(\omega_1^2 + 2\omega_2^2\right) - 3\alpha_4\right] A_1 A_2 \bar{A}_2 = 0 \end{aligned} \tag{50}$$

$$\begin{aligned} &2i\omega_2 \left(2\omega_2^2 - \alpha_1\right) D_2 A_2 + 3\left(\alpha_2 \omega_2^2 - \alpha_4\right) A_2^2 \bar{A}_2 \\ &\quad + 2\left[\alpha_2 \left(\omega_2^2 + 2\omega_1^2\right) - 3\alpha_4\right] A_1 \bar{A}_1 \bar{A}_2 = 0 \end{aligned} \tag{51}$$

In solving Eqs. (47) and (48), A_1 and A_2 are expressed in polar form

$$A_1 = \frac{1}{2} a_1 e^{ib_1}; \quad A_2 = \frac{1}{2} a_2 e^{ib_2} \tag{52}$$

where $a_j\,(j=1,2)$ and $b_j\,(j=1,2)$ are real functions of T_2. Substituting Eq. (49) into Eq. (48) and separating the result into real and imaginary parts in each and then solving the resulting differential equations, it follows that a_1 and a_2 are constants and $b_j\,(j=1,2)$ are given by

$$b_1=\delta_1 T_2+\beta_{10};\quad b_2=\delta_2 T_2+\beta_{20} \tag{53}$$

where β_{10} and β_{20} are constants and

$$\delta_1=\frac{3\left(\alpha_2\omega_1^2-\alpha_4\right)a_1^2+2\left[\alpha_2\left(\omega_1^2+2\omega_2^2\right)-3\alpha_4\right]a_2^2}{8\omega_1\left(2\omega_1^2-\alpha_1\right)} \tag{54}$$

$$\delta_2=\frac{3\left(\alpha_2\omega_2^2-\alpha_4\right)a_2^2+2\left[\alpha_2\left(\omega_2^2+2\omega_1^2\right)-3\alpha_4\right]a_1^2}{8\omega_2\left(2\omega_2^2-\alpha_1\right)} \tag{55}$$

Now, by substituting $\delta_j\ (j=1,2)$ from Eqs. (51) and (52) into Eq. (49), A_1 and A_2 are obtained as

$$A_1=\frac{1}{2}a_1\exp\left[i\varepsilon^2\delta_1 t+i\beta_{10}\right] \tag{56}$$

$$A_2=\frac{1}{2}a_2\exp\left[i\varepsilon^2\delta_2 t+i\beta_{20}\right] \tag{57}$$

where $T_2=\varepsilon^2\,t$ is used.

To this end, one solves for q_3 with retaining only the particular solution and then combines the resulting expression with q_1 from Eq. (43) according to Eq. (39) and noting that $q_2=0$, to arrive at the following uniformly valid expression for q in real functional forms after accounting for the complex conjugate.

$$\begin{aligned}q=&\,\varepsilon\{a_1Cos(\Omega_1 t+\beta_{10})+a_2Cos(\Omega_2 t+\beta_{20})\}\\&+\varepsilon^3\left\{\begin{array}{l}C_1a_1^3Cos(3\Omega_1 t+3\beta_{10})+C_2a_2^3Cos(3\Omega_2 t+3\beta_{20})\\+C_3a_1a_2^2Cos[(\Omega_1+2\Omega_2)t+\beta_{10}+2\beta_{20}]\\+C_4a_1a_2^2Cos[(\Omega_1-2\Omega_2)t+\beta_{10}-2\beta_{20}]\\+C_5a_1^2a_2Cos[(2\Omega_1+\Omega_2)t+2\beta_{10}+\beta_{20}]\\+C_6a_1^2a_2Cos[(2\Omega_1-\Omega_2)t+2\beta_{10}-\beta_{20}]\end{array}\right\}\end{aligned} \tag{58}$$

where the nonlinear frequencies Ω_j are given by

$$\Omega_j=\omega_j+\varepsilon^2\delta_j+O\left(\varepsilon^3\right);\quad j=1,2 \tag{59}$$

and the coefficients $C_j, j=1-6$ are

$$\begin{aligned}C_1&=\frac{\alpha_2\omega_1^2-\alpha_4}{4\left(81\omega_1^4-9\alpha_1\omega_1^2+\alpha_3\right)};\\C_2&=\frac{\alpha_2\omega_2^2-\alpha_4}{4\left(81\omega_2^4-9\alpha_1\omega_2^2+\alpha_3\right)};\\C_3&=\frac{\alpha_2\left(\omega_1^2+2\omega_2^2\right)-3\alpha_4}{4\left((\omega_1+2\omega_2)^4-\alpha_1(\omega_1+2\omega_2)^2+\alpha_3\right)};\\C_4&=\frac{\alpha_2\left(\omega_1^2+2\omega_2^2\right)-3\alpha_4}{4\left((\omega_1-2\omega_2)^4-\alpha_1(\omega_1-2\omega_2)^2+\alpha_3\right)};\\C_5&=\frac{\alpha_2\left(\omega_2^2+2\omega_1^2\right)-3\alpha_4}{4\left((2\omega_1+\omega_2)^4-\alpha_1(2\omega_1+\omega_2)^2+\alpha_3\right)};\\C_6&=\frac{\alpha_2\left(\omega_2^2+2\omega_1^2\right)-3\alpha_4}{4\left((2\omega_1-\omega_2)^4-\alpha_1(2\omega_1-\omega_2)^2+\alpha_3\right)};\end{aligned} \tag{60}$$

Applying initial conditions, Eq. (38), leads to

$$\begin{aligned}&a_1=\frac{\omega_2^2W_{\max}}{\left(\omega_2^2-\omega_1^2\right)L};\quad a_2=\frac{\omega_1^2W_{\max}}{\left(\omega_1^2-\omega_2^2\right)L};\\&\beta_{10}=\beta_{20}=0\end{aligned} \tag{61}$$

It is to be pointed out that the small parameter ε which has now served its purpose may be set equal to 1. It may be further noted that the simply supported Euler–Bernoulli nanobeam nondimensional nonlinear frequency can be recovered by setting, separately, $\omega=(n\pi/L)^2\sqrt{EI/\rho A}$, $\rho I=0$ (i.e. no rotational inertia) and $KAG=0$ (no shear deformation) in the expression for Ω_1 given by Eq. (56). This gives

$$\Omega_{nl(EB)}=\sqrt{\beta_1^{EB}}\left(1+\frac{3}{8}\left(\frac{\beta_2^{EB}}{\beta_1^{EB}}W_{\max}^2\right)\right) \tag{62}$$

where $\beta_{1,2}^{EB}$ are given in "Appendix".

Here, it is also worthwhile to point out that it is possible to introduce an exact solution for nonlinear free vibration of Euler–Bernoulli nanobeams incorporating the surface energy using elliptic integrals [46]. To this end, neglecting rotational inertia and shear deformation terms, ρI and KAG, respectively, assuming $W(x,t)=D\Phi(x)q(t)$ for the transverse displacement and using the averaging technique over the space variable lead to

$$\ddot{q}+\chi_1 q+\chi_2 q^3=0 \tag{63}$$

The parameters $\chi_{1,2}$ are given in Ref. [46]. Using elliptic integrals, the solution of Eq. (63) leading the

nonlinear natural frequencies of Euler–Bernoulli nanobeam is given by

$$\omega_{nl(\mathrm{E-B})} = \frac{\pi\sqrt{\chi_1 + \chi_2}}{2K} \tag{64}$$

where $\mathrm{K} = \int_0^{\pi/2} \frac{d\theta}{\sqrt{1-\kappa^2 Sin^2(\theta)}}$ and $\kappa^2 = \frac{\chi_2}{2(\chi_1+\chi_2)}$.

4 Results and discussion

4.1 Comparison study

To confirm the reliability of the present formulation and results, two comparison study are conducted for the frequency ratios of linear Euler–Bernoulli and Timoshenko nanobeams in the presence of the surface energy with different boundary conditions [43] and the frequency ratios of a nonlinear simply supported Euler–Bernoulli nanobeam in the presence of the surface energy [46].

Table 1 gives a comparison between the present results obtained by the method of multiple scales with those obtained by the closed-form analytical solution [43] for the linear natural frequencies of Euler–Bernoulli and Timoshenko nanobeams incorporating the surface energy when the balance condition is satisfied. In Table 1, the results are listed for nanobeams made of aluminum and silicon with three different boundary conditions. The material properties and dimensions of the nanobeams are chosen as Ref. [43]. It is seen from Table 1 that the present results obtained by the multiple scale methods are in excellent agreement with those reported by Liu and Rajapakse [43] using the closed-form analytical solution.

Fundamental nonlinear natural frequency ratios of a SS Euler–Bernoulli nanobeam with the surface energy are given in Table 2. The exact results reported by Nazemnezhad et al. [46] are also provided for direct comparison. Table 2 shows that the present results obtained by the multiple scale method are identical to those reported in Ref. [46] using the exact solution. However, the difference between two solutions increases as the vibration amplitude increases. This is due to the fact that the accuracy of the multiple scale method, especially at higher vibration amplitude, depends on the number of slow scale variables in the expansion series.

4.2 Benchmark results

To demonstrate the influences of the balance condition and the surface density in addition to the surface elasticity and stress on the nonlinear free vibration of nanobeams, variations of the frequency ratios, Eq. (62), versus vibration amplitude and dimensions

Table 1 Comparison of linear natural frequencies (GHz)

Nanobeam type		First		Second		Third		Forth	
		Present	Ref. [39]	Present	Ref. [39]	Present	Ref. [39]	Present	Ref. [39]
Aluminum nanobeam									
EBT	SS	1.4508	1.45	4.4687	4.47	9.3945	9.39	16.2717	16.27
	SC	1.9155	–	5.4433	–	10.8758	–	11.4697	–
	CC	2.5219	2.52	6.5498	6.37	12.4862	12.49	20.3642	20.35
TBT	SS	6.0878	6.10	21.4599	21.49	43.9565	43.96	71.0868	71.08
	SC	8.8467	–	25.8738	–	48.9913	–	76.0273	–
	CC	12.1751	12.18	30.3974	30.40	53.9285	53.92	80.7720	80.85
Silicon nanobeam									
EBT	SS	1.6619	1.66	5.1883	5.19	10.9587	10.96	19.0188	19.02
	SC	2.2118	–	6.3361	–	12.6997	–	21.3468	–
	CC	2.9289	2.94	7.6382	7.64	14.5915	14.59	23.8231	23.83
TBT	SS	7.0824	7.08	25.0687	25.07	51.3388	51.33	82.9402	82.92
	SC	10.3139	–	30.1861	–	57.1058	–	88.5195	–
	CC	14.1978	14.20	35.4066	35.41	62.7372	62.74	93.8602	93.86

Table 2 Comparison of frequency ratios for Euler–Bernoulli nanobeam

q_{max}/r	SS			SC			CC		
	Exact [42]	Present (MS*)	Diff. (%)	Exact [42]	Present (MS)	Diff. (%)	Exact [42]	Present (MS)	Diff. (%)
0.0	1.1540	1.1540	0.00	1.0826	1.0826	0.00	1.0492	1.0492	0.00
0.5	1.1472	1.1471	0.02	1.0805	1.0804	0.00	1.0478	1.0478	0.00
1.0	1.1302	1.1281	0.20	1.0746	1.0742	0.04	1.0439	1.0436	0.03
1.5	1.1091	1.1015	0.76	1.0666	1.0648	0.17	1.0386	1.0374	0.12
2.0	1.0888	1.0718	1.70	1.0577	1.0534	0.43	1.0328	1.0298	0.30
2.5	1.0714	1.0427	2.87	1.0491	1.0409	0.82	1.0273	1.0215	0.57
3.0	1.0517	1.0161	4.10	1.0413	1.0282	1.30	1.0223	1.0133	0.90
3.5	1.0458	0.9930	5.29	1.0344	1.0161	1.83	1.0180	1.0054	1.26
4.0	1.0369	0.9732	6.36	1.0286	1.0049	2.37	1.0143	0.9982	1.62

* Multiple scale solution

of the nanobeam for SS, SC and CC boundary conditions are considered graphically in this section. Some selected data from each graph are also presented in tabular form as benchmark. For the brevity, SC, for example, denotes that one end of the nanobeam is simply supported and the other one is clamped. A nanobeam made of aluminum (Al) with crystallographic direction of [111] is considered as illustrative example. The bulk elastic properties are $E = 70$ GPa, $v = 0.35$, $\rho = 2{,}700$ kg/m^3, $G = E/(2(1 + v))$ [68] and the surface elastic properties are $E^s = 5.1882$ N/m, $\tau_0 = 0.9108$ N/m, $\rho_0 = 5.46e{-}7$ [69]. We know that the influence of the shear deformation becomes important when the length to depth ratio of a nanoscale beam is smaller than 10; thus the cross section of the nanobeam is set to be square with $b = 2h = L/8$ and the shear correction factor is considered to be 5/6 [70]. In the following discussion, Case-1 denotes the natural frequencies of nanobeams obtained by considering all components of the surface energy as well as satisfying the balance condition between the nanobeams bulk and their surfaces, and Case-2 represents the natural frequencies of nanobeams obtained by considering only the surface elasticity and stress effects.

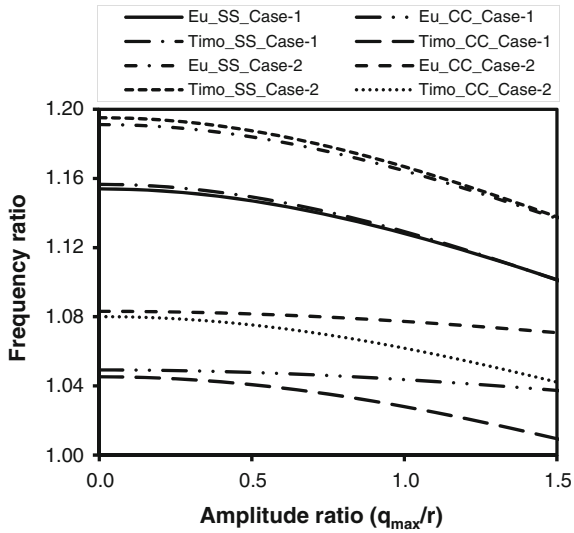

Fig. 2 Variations of the frequency ratios versus the amplitude ratio

comparison, the frequency ratios of nanobeams with only the SS and CC boundary conditions are presented in Fig. 2. The frequency ratios of Timoshenko and

$$Frequency\ ratio = \frac{Natural\ frequency\ with\ the\ surface\ energy\ and\ the\ balance\ condition}{Natural\ frequency\ without\ the\ surface\ energy\ and\ the\ balance\ condition} \tag{65}$$

Firstly, the variations of the frequency ratios versus the amplitude ratio are plotted in Fig. 2 when b = 2h = L/8 and L = 50 nm. For the sake of Euler–Bernoulli nanobeams with all types of mentioned boundary conditions for both Case-1 and Case-2 are also listed in Table 3 as the benchmark. It is seen

Table 3 Linear and nonlinear frequency ratios of Euler–Bernoulli (EBT) and Timoshenko (TBT) nanobeams for various amplitude ratios (q_{max}/r), $b = 2h = L/8$

Amplitude ratio	SS				SC				CC			
	Case-1		Case-2		Case-1		Case-2		Case-1		Case-2	
	EBT	TBT	EBT	TBT	EBT	TBT	EBT	TBT	EBT	TBT	EBT	TBT
0.00	1.154	1.157	1.191	1.195	1.083	1.083	1.118	1.119	1.049	1.045	1.083	1.080
0.30	1.151	1.154	1.189	1.192	1.082	1.082	1.117	1.118	1.049	1.044	1.083	1.078
0.60	1.144	1.146	1.181	1.184	1.080	1.079	1.114	1.114	1.047	1.039	1.081	1.073
0.90	1.133	1.134	1.169	1.172	1.076	1.073	1.110	1.109	1.045	1.031	1.078	1.065
1.20	1.118	1.119	1.154	1.156	1.071	1.067	1.105	1.102	1.041	1.021	1.075	1.055
1.50	1.101	1.101	1.137	1.138	1.065	1.059	1.099	1.094	1.037	1.009	1.071	1.042

from Fig. 2 that all the curves show values more than 1, indicating that the surface energy causes an increase in the natural frequencies of the nanobeams. Furthermore, all the frequency ratios exhibit a decreasing trend as the amplitude ratio (q_{max}/r) increases. In other words, as the vibration of nanobeam approaches the nonlinear behavior, the effects of the surface energy on the natural frequency decrease. Moreover, this reduction becomes more pronounced for nanobeams with softer boundary condition, i.e. SS end condition.

Figure 2 shows that the frequency ratio curves in Case-2 are located above those in Case-1, implying that considering the surface density effect and satisfying the balance condition between the nanobeam bulk and its surfaces cause a reduction in the frequency ratios. This reduction is a little more for Timoshenko nanobeams than Euler–Bernoulli ones for all types of boundary conditions.

Making a comparison between Euler–Bernoulli and Timoshenko curves shows that the influences of the surface energy on the linear natural frequency differ from the nonlinear one and the differences depends on the nanobeam boundary conditions. In the case of linear vibration, the increasing effect of the surface energy on the natural frequencies of the SS Timoshenko nanobeam is a little more than the SS Euler–Bernoulli one while this conclusion is the other way round for the CC boundary condition. By increasing the vibration amplitude, accordingly increasing the nonlinearity, the frequency ratio curves of SS Euler–Bernoulli and Timoshenko nanobeams approach each other whereas the distance between those of CC Euler–Bernoulli and Timoshenko nanobeams becomes more.

As a general conclusion, using higher restraining boundary conditions results in this fact that considering the rotary inertia and shear deformation causes further reductions in the surface energy effects. This is true for both the linear and nonlinear vibrations while intensity of the reduction is more for the nonlinear case.

Next, the variations of the linear and nonlinear frequency ratios versus the nanobeam length are displayed in Fig. 3a–d for SS and CC boundary conditions. Here, the results of the SC boundary condition as well as the SS and CC boundary conditions are given in Tables 4 and 5. In Fig. 3a, b, the nanobeam cross section is considered to be dependent on the nanobeam length, $b = 2h = L/8$, whereas in Fig. 3c, d, the nanobeam cross section is considered to be constant, $b = 2h = 10$ nm. Fig. 3a–d not only reconfirm the mentioned remarks for Fig. 2 but also make the following new results:

- When the nanobeam cross section depends on its length, the surface energy effects on the natural frequencies decrease as the length of nanobeam increases. This is due to this fact that as the nanobeam goes to the thicker and longer one, the energy stored in the surfaces decreases in comparison with the energy stored in the bulk.
- When the nanobeam cross section is set to be constant, the effects of the surface energy on the natural frequencies increase by increasing the nanobeam length. Unlike the previous case, this

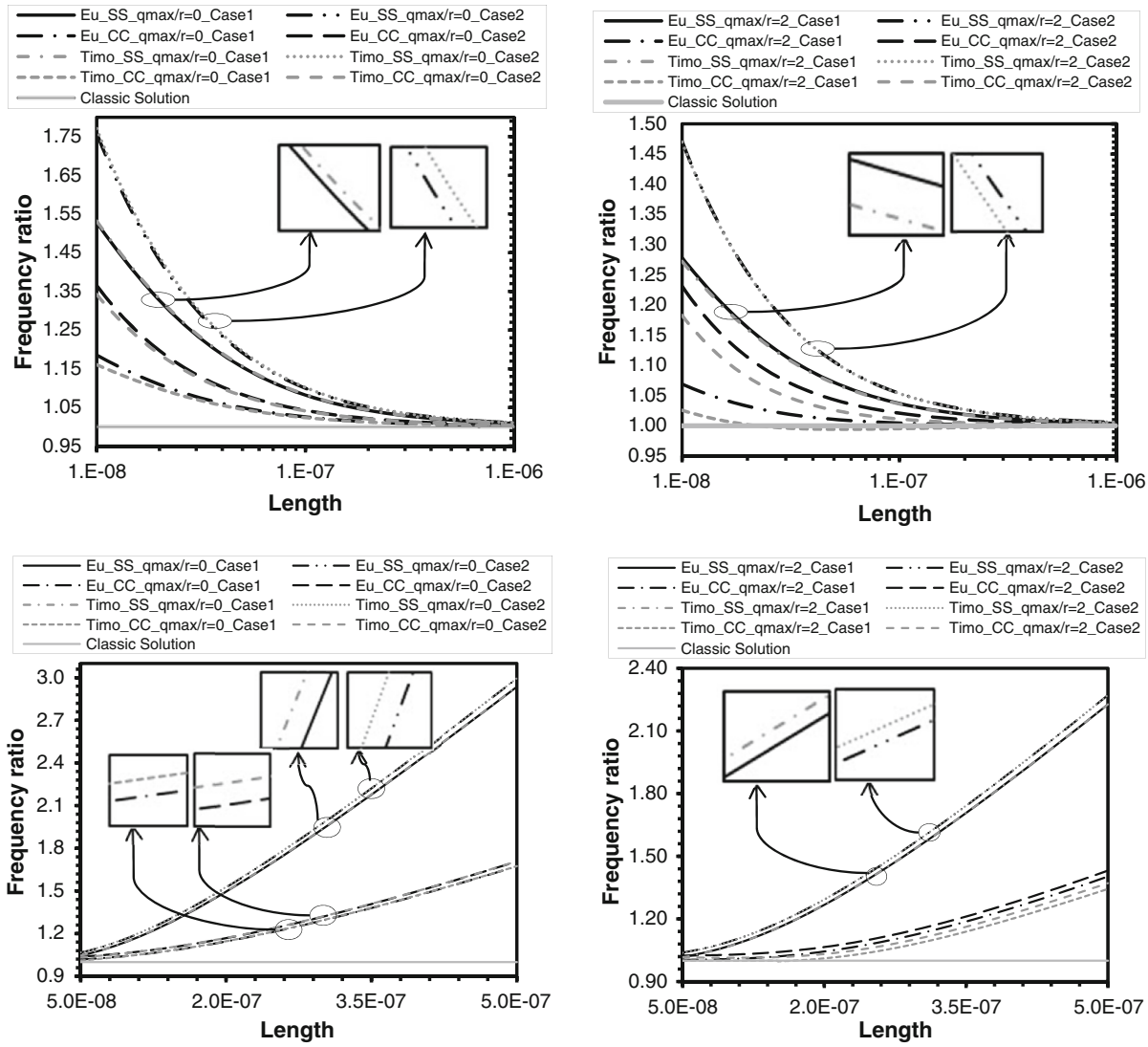

Fig. 3 Variations of the linear and nonlinear frequency ratios versus the length of nanobeam, **a** linear frequencies with b = 2h = L/8, **b** nonlinear frequencies with b = 2h = L/8, **c** linear frequencies with b = 2h = 10 nm, **d** nonlinear frequencies with b = 2h = 10 nm

is because of an increase in the surface energy-to-bulk energy ratio.

Lastly, in Fig. 4a, b, the variations of the linear and nonlinear frequency ratios as a function of the thickness ratio (2h/L) are presented when b = 2h and L = 50 nm. A numerical comparison between the frequency ratios of Timoshenko and Euler–Bernoulli nanobeams with three different boundary conditions is also conducted in Table 6. It is observed from Fig. 4a, b and Table 6 that as the thickness ratio increases, the surface energy effects on the natural frequencies decrease. This trend is true for both the linear and nonlinear vibrations of nanobeams. In addition, it can be concluded from Fig. 4a that for all values of the thickness ratio the surface energy shows similar effects on the linear frequency ratios of both

Table 4 Linear and nonlinear frequency ratios of Euler–Bernoulli (EBT) and Timoshenko (TBT) nanobeams for different nanobeam lengths when b = 2h = L/8

q_{max}/r	Length (nm)	SS				SC				CC			
		Case-1		Case-2		Case-1		Case-2		Case-1		Case-2	
		EBT	TBT	EBT	TBT	EBT	TBT	EBT	TBT	EBT	TBT	EBT	TBT
0.0	10	1.528	1.532	1.759	1.771	1.300	1.291	1.497	1.493	1.185	1.161	1.366	1.342
	25	1.275	1.279	1.356	1.362	1.151	1.149	1.224	1.225	1.091	1.082	1.160	1.153
	50	1.154	1.157	1.191	1.195	1.083	1.083	1.118	1.119	1.049	1.045	1.083	1.080
	100	1.082	1.084	1.100	1.102	1.044	1.044	1.061	1.061	1.026	1.024	1.042	1.041
	500	1.017	1.018	1.021	1.021	1.009	1.009	1.012	1.013	1.005	1.005	1.009	1.008
	1,000	1.009	1.009	1.010	1.011	1.005	1.005	1.006	1.006	1.003	1.002	1.004	1.004
2.0	10	1.278	1.272	1.471	1.470	1.189	1.170	1.369	1.352	1.069	1.026	1.231	1.183
	25	1.135	1.132	1.206	1.206	1.090	1.082	1.159	1.152	1.025	0.998	1.090	1.061
	50	1.072	1.070	1.106	1.106	1.048	1.044	1.082	1.078	1.011	0.994	1.043	1.026
	100	1.037	1.036	1.054	1.053	1.025	1.022	1.041	1.040	1.005	0.995	1.021	1.011
	500	1.008	1.007	1.011	1.011	1.005	1.005	1.008	1.008	1.001	0.999	1.004	1.002
	1,000	1.004	1.004	1.005	1.005	1.003	1.002	1.004	1.004	1.000	0.999	1.002	1.001

Table 5 Linear and nonlinear frequency ratios of Euler–Bernoulli (EBT) and Timoshenko (TBT) nanobeams for different nanobeam lengths when b = 2h = 10 nm

q_{max}/r	Length (nm)	SS				SC				CC			
		Case-1		Case-2		Case-1		Case-2		Case-1		Case-2	
		EBT	TBT	EBT	TBT	EBT	TBT	EBT	TBT	EBT	TBT	EBT	TBT
0.0	50	1.046	1.045	1.067	1.068	1.027	1.023	1.047	1.045	1.018	1.010	1.038	1.032
	100	1.150	1.152	1.173	1.176	1.078	1.079	1.100	1.102	1.045	1.044	1.066	1.065
	200	1.495	1.497	1.525	1.527	1.262	1.265	1.288	1.290	1.145	1.146	1.168	1.170
	300	1.938	1.940	1.977	1.979	1.517	1.519	1.548	1.550	1.293	1.295	1.319	1.321
	400	2.425	2.427	2.474	2.476	1.811	1.812	1.847	1.849	1.473	1.474	1.503	1.505
	500	2.936	2.937	2.995	2.996	2.125	2.126	2.168	2.169	1.673	1.675	1.707	1.709
2.0	50	1.019	1.016	1.039	1.038	1.015	1.009	1.035	1.030	1.004	1.000	1.024	1.016
	100	1.071	1.070	1.092	1.092	1.046	1.044	1.067	1.065	1.008	1.000	1.029	1.014
	200	1.268	1.268	1.293	1.294	1.168	1.167	1.191	1.191	1.044	1.011	1.065	1.032
	300	1.548	1.549	1.580	1.580	1.352	1.352	1.380	1.380	1.129	1.084	1.152	1.106
	400	1.875	1.876	1.913	1.913	1.576	1.577	1.608	1.608	1.254	1.202	1.279	1.227
	500	2.227	2.228	2.272	2.272	1.823	1.824	1.860	1.860	1.403	1.344	1.432	1.371

nanobeam types. However, it should be noted that according to Fig. 3a–d, this conclusion depends on the nanobeam length. Whereas, Fig. 4b displays that if the nanobeam be thicker and has stiffer boundary conditions, considering rotary inertia and shear deformation leads to a more reduction the surface energy effects on the nonlinear natural frequencies. A final point to note is that for all values of the thickness ratio, the nonlinear frequency ratios are smaller than the linear ones, indicating that the surface energy has more

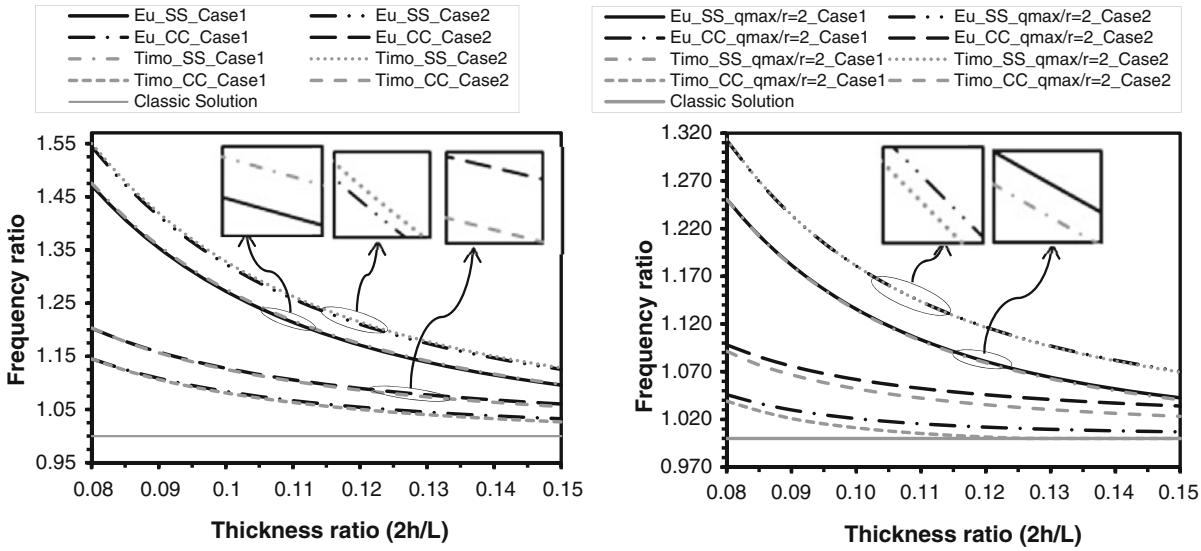

Fig. 4 Variations of the frequency ratios versus the nanobeam thickness ratio when the length of nanobeam is set to be 50 nm, **a** linear frequency ratios, **b** Nonlinear frequency ratios with $q_{max}/r = 2$

Table 6 Linear and nonlinear frequency ratios of Euler–Bernoulli (EBT) and Timoshenko (TBT) nanobeams for various thickness ratios (2h/L)

q_{max}/r	Thickness ratio	SS				SC				CC			
		Case-1		Case-2		Case-1		Case-2		Case-1		Case-2	
		EBT	TBT	EBT	TBT	EBT	TBT	EBT	TBT	EBT	TBT	EBT	TBT
0.0	0.08	1.471	1.476	1.544	1.550	1.254	1.257	1.317	1.321	1.145	1.145	1.203	1.203
	0.10	1.272	1.276	1.323	1.328	1.145	1.147	1.191	1.194	1.084	1.081	1.128	1.126
	0.12	1.171	1.174	1.210	1.215	1.092	1.092	1.128	1.130	1.054	1.050	1.090	1.086
	0.14	1.115	1.117	1.147	1.150	1.062	1.061	1.093	1.093	1.038	1.033	1.068	1.064
	0.15	1.096	1.097	1.125	1.128	1.053	1.051	1.081	1.080	1.033	1.027	1.060	1.056
2.0	0.08	1.251	1.250	1.313	1.313	1.161	1.158	1.219	1.217	1.046	1.039	1.098	1.091
	0.10	1.135	1.135	1.181	1.181	1.088	1.083	1.131	1.127	1.021	1.011	1.062	1.052
	0.12	1.081	1.079	1.117	1.116	1.054	1.049	1.089	1.085	1.012	1.002	1.046	1.035
	0.14	1.052	1.050	1.082	1.081	1.036	1.030	1.065	1.061	1.008	1.000	1.037	1.026
	0.15	1.043	1.041	1.070	1.070	1.030	1.024	1.057	1.053	1.007	1.000	1.034	1.023

influences on natural frequencies in the case of linear vibration than the nonlinear one. The mentioned remarks are valid for both the Case-1 and the Case-2.

5 Conclusion

In this paper, the influences of the balance condition and the surface density in addition to the surface elasticity and stress on the nonlinear free vibration of Timoshenko and Euler–Bernoulli nanobeams are investigated. In order to consider the balance condition between the nanobeam bulk and its surfaces, it is assumed that the normal stress, σ_{zz}, varies linearly along the nanobeam thickness. Accordingly, the surface density in addition to the surface stress and elasticity is introduced into the governing equations of the nonlinear free vibration of nanobeams. Moreover, besides using the bulk density, the surface density is also employed to obtain the kinetic energy of the

nanobeams. Closed-form solution for the nonlinear natural frequencies of the nanobeams is obtained using the method of multiple scales. The following conclusions could be highlighted from this study:

- Considering the surface density effect and satisfying the balance condition cause a reduction in the frequency ratios, and this reduction is a little more for Timoshenko nanobeams than Euler–Bernoulli ones for all types of boundary conditions used.
- As the vibration of nanobeam approaches the nonlinear behavior, the effects of the surface energy on the natural frequency decrease. Moreover, this reduction becomes more pronounced for nanobeams with softer boundary condition, i.e. SS end condition.
- If the nanobeam cross section is dependent to its length, the surface energy effects on the natural frequencies decrease as the length of nanobeam increases. This situation is the other way round when the nanobeam cross section is independent of its length.

Appendix

- The variables used in Eq. (30) for a Timoshenko nanobeam

$$\begin{cases} S_1 = \sqrt{\left(\left(-(\rho I)^{**}\Omega_{L(T)}^2 + H\right) + \sqrt{\left(-(\rho I)^{**}\Omega_{L(T)}^2 + H\right)^2 - 4(EI)^*\left(\lambda\Omega_{L(T)}^4 - mL\omega^2\Omega_{L(T)}^2\right)}\right)\Big/2(EI)^*} \\ S_2 = \sqrt{\left(-\left(-(\rho I)^{**}\Omega_{L(T)}^2 + H\right) + \sqrt{\left(-(\rho I)^{**}\Omega_{L(T)}^2 + H\right)^2 - 4(EI)^*\left(\lambda\Omega_{L(T)}^4 - mL\omega^2\Omega_{L(T)}^2\right)}\right)\Big/2(EI)^*} \end{cases}$$

$$\begin{cases} \zeta_1 = \sqrt{\left(\kappa_2 + \sqrt{\kappa_2^2 - 4\kappa_1\kappa_3}\right)\Big/2\kappa_1} \\ \zeta_2 = \sqrt{\left(-\kappa_2 + \sqrt{\kappa_2^2 - 4\kappa_1\kappa_3}\right)\Big/2\kappa_1} \end{cases}$$

$$\begin{cases} \kappa_1 = kAG\left(\tau_0 \upsilon I/h - (1 + 2b\tau_0/kAG)\left(EI + E^s\left(4h^3/3 + 2bh^2\right)\right)\right)/L^3; \\ \kappa_2 = kAG\left(\left(\rho_0 \upsilon IL\omega^2/h - kAG\right) - (1 + 2b\tau_0/kAG)\left(kAG + (\rho I)^*\omega^2\Omega_{L(T)}^2\right)\right)\Big/L \\ \qquad - \left(mL\omega^2\Omega_{L(T)}^2\right)\left(EI + E^s\left(4h^3/3 + 2bh^2\right)\right)\Big/L^2; \\ \kappa_3 = \left(mL\omega^2\Omega_{L(T)}^2\right)\left(kAG - (\rho I)^*\omega^2\Omega_{L(T)}^2\right); \end{cases}$$

$$\begin{cases} K_a = \left((kAG + 2b\tau_0)\zeta_1^2 - mL^2\omega^2\Omega_{L(T)}^2\right)\Big/kAG\zeta_1; \\ K_b = \left((kAG + 2b\tau_0)\zeta_2^2 + mL^2\omega^2\Omega_{L(T)}^2\right)\Big/kAG\zeta_2; \end{cases}$$

- Using higher restraining boundary conditions results in this fact that considering the rotary inertia and shear deformation causes reductions in the surface energy effects. This is true for both the linear and nonlinear vibrations while intensity of the reduction is more for the nonlinear case.

where $\Omega_{L(T)}$ is the linear natural frequency of Timoshenko nanobeams when all the components of the surface energy as well as the balance condition are considered.

- The variables used in Eq. (62) for an Euler–Bernoulli nanobeam

$$
\begin{cases}
\beta_1^{EB} = \dfrac{(EI)^*_{EB} a_4^{EB} + LH^{EB} a_3^{EB}}{\upsilon\rho_0 I a_3^{EB}/h + m a_1^{EB}}; \quad \beta_2^{EB} = \dfrac{-P a_2^{EB} a_3^{EB}}{\left(\upsilon\rho_0 I a_3^{EB}/h + m a_1^{EB}\right) L}; \\
(EI)^*_{EB} = EI + E^s\left(\dfrac{4h^3}{3} + 2bh^2\right) - \dfrac{vI\tau_0}{h}; \\
a_1^{EB} = \int_0^L \left(\phi_{EB}^2\right) dx; \quad a_2^{EB} = \int_0^L \left(\dfrac{d\phi_{EB}}{dx}\right)^2 dx; \quad a_3^{EB} = \int_0^L \left(\phi_{EB} \cdot \dfrac{d^2\phi_{EB}}{dx^2}\right) dx; \quad a_4^{EB} = \int_0^L \left(\phi_{EB} \cdot \dfrac{d^4\phi_{EB}}{dx^4}\right) dx;
\end{cases}
$$

$$
\begin{cases}
\phi_{SS}^{EB} = Sin\left(\dfrac{n\pi x}{L}\right), \quad n = 1, 2, 3, \ldots; \\
\phi_{SC}^{EB} = Sin\left(S_1^{EB} x\right) - \dfrac{Sin\left(S_1^{EB} L\right)}{Sinh\left(S_2^{EB} L\right)} Sinh\left(S_2^{EB} x\right); \Rightarrow \; ChEq: \; S_2^{EB} Tan\left(S_1^{EB}\right) - S_1^{EB} Tanh\left(S_2^{EB}\right) = 0 \\
\phi_{CC}^{EB} = Sin\left(S_1^{EB} x\right) - \dfrac{S_1^{EB}}{S_2^{EB}} Sinh\left(S_2^{EB} x\right) - \dfrac{Sin\left(S_1^{EB} L\right) - \left(S_1^{EB}/S_2^{EB}\right) Sinh\left(S_2^{EB} L\right)}{Cos\left(S_1^{EB} L\right) - Cosh\left(S_2^{EB} L\right)} \left(Cos\left(S_1^{EB} x\right) - Cosh\left(S_2^{EB} x\right)\right); \\
\quad \Rightarrow \; ChEq: \; 2S_1^{EB} S_2^{EB} \left(Cos\left(S_1^{EB}\right) Cosh\left(S_2^{EB}\right) - 1\right) + \left(\left(S_1^{EB}\right)^2 - \left(S_2^{EB}\right)^2\right) Sin\left(S_1^{EB}\right) Sinh\left(S_2^{EB}\right) = 0
\end{cases}
$$

$$
\begin{cases}
S_1 = \sqrt{\left(\left(-(\upsilon\rho_0 I/h)\Omega_{L(EB)}^2 + H^{EB}\right) + \sqrt{\left(-(\upsilon\rho_0 I/h)\Omega_{L(EB)}^2 + H^{EB}\right)^2 + 4(EI)^*\left(m\Omega_{L(EB)}^2\right)}\right) \Big/ 2(EI)^*} \\
S_2 = \sqrt{\left(-\left(-(\upsilon\rho_0 I/h)\Omega_{L(EB)}^2 + H^{EB}\right) + \sqrt{\left(-(\upsilon\rho_0 I/h)\Omega_{L(EB)}^2 + H^{EB}\right)^2 + 4(EI)^*\left(m\Omega_{L(EB)}^2\right)}\right) \Big/ 2(EI)^*}
\end{cases}
$$

where $\Omega_{L(EB)}$ is the linear natural frequency of Euler–Bernoulli nanobeams when all the components of the surface energy as well as the balance condition are considered.

References

1. Evoy S, Carr D, Sekaric L, Olkhovets A, Parpia J, Craighead H (1999) Nanofabrication and electrostatic operation of single-crystal silicon paddle oscillators. J Appl Phys 86(11):6072–6077
2. Lavrik NV, Sepaniak MJ, Datskos PG (2004) Cantilever transducers as a platform for chemical and biological sensors. Rev Sci Instrum 75(7):2229–2253
3. Gurtin ME, Murdoch AI (1975) A continuum theory of elastic material surfaces. Arch Ration Mech Anal 57(4):291–323
4. Gurtin M, Weissmüller J, Larche F (1998) A general theory of curved deformable interfaces in solids at equilibrium. Philos Mag A 78(5):1093–1109
5. Lü C, Chen W, Lim C (2009) Elastic mechanical behavior of nano-scaled FGM films incorporating surface energies. Compos Sci Technol 69(7):1124–1130
6. Lü C, Lim C, Chen W (2009) Size-dependent elastic behavior of FGM ultra-thin films based on generalized refined theory. Int J Solids Struct 46(5):1176–1185
7. Lu P, He L, Lee H, Lu C (2006) Thin plate theory including surface effects. Int J Solids Struct 43(16):4631–4647
8. Zhang J-H, Huang Q-A, Yu H, Wang J (2009) The influence of surface effects on size-dependent mechanical properties of silicon nanobeams at finite temperature. J Phys D Appl Phys 42(4):045409
9. Sadeghian H, Goosen H, Bossche A, Thijsse B, van Keulen F (2011) On the size-dependent elasticity of silicon nanocantilevers: impact of defects. J Phys D Appl Phys 44(7):072001
10. Guo J-G, Zhao Y-P (2007) The size-dependent bending elastic properties of nanobeams with surface effects. Nanotechnology 18(29):295701
11. Bar On B, Altus E, Tadmor E (2010) Surface effects in non-uniform nanobeams: continuum vs. atomistic modeling. Int J Solids Struct 47(9):1243–1252
12. Zheng X-P, Cao Y-P, Li B, Feng X-Q, Wang G-F (2010) Surface effects in various bending-based test methods for measuring the elastic property of nanowires. Nanotechnology 21(20):205702
13. Wang J-S, Cui Y-H, Feng X-Q, Wang G-F, Qin Q-H (2010) Surface effects on the elasticity of nanosprings. Europhys Lett 92(1):16002
14. Xia R, Li X, Qin Q, Liu J, Feng X-Q (2011) Surface effects on the mechanical properties of nanoporous materials. Nanotechnology 22(26):265714
15. Wang J-S, Wang G-F, Feng X-Q, Qin Q-H (2012) Surface effects on the superelasticity of nanohelices. J Phys Condens Matter 24(26):265303

16. Assadi A, Farshi B (2011) Size-dependent longitudinal and transverse wave propagation in embedded nanotubes with consideration of surface effects. Acta Mech 222(1–2):27–39
17. Narendar S, Ravinder S, Gopalakrishnan S (2012) Study of non-local wave properties of nanotubes with surface effects. Comput Mater Sci 56:179–184
18. Velasco V, Garcia-Moliner F (1979) Surface effects in elastic surface waves. Phys Scripta 20(1):111
19. Wang Q (2005) Wave propagation in carbon nanotubes via nonlocal continuum mechanics. J Appl Phys 98(12):124301
20. Ma JB, Jiang L, Asokanthan SF (2010) Influence of surface effects on the pull-in instability of NEMS electrostatic switches. Nanotechnology 21(50):505708
21. Rokni H, Seethaler RJ, Milani AS, Hosseini-Hashemi S, Li X-F (2013) Analytical closed-form solutions for size-dependent static pull-in behavior in electrostatic micro-actuators via Fredholm integral method. Sens Actuator A Phys 190:32–43
22. Fu Y, Zhang P (2010) Buckling and vibration of core–shell nanowires with weak interfaces. Mech Res Commun 37(7):622–626
23. Wang G-F, Feng X-Q (2009) Timoshenko beam model for buckling and vibration of nanowires with surface effects. J Phys D Appl Phys 42(15):155411
24. Wang Y, Song J, Xiao J (2013) Surface effects on in-plane buckling of nanowires on elastomeric substrates. J Phys D Appl Phys 46(12):125309
25. Li Y, Song J, Fang B, Zhang J (2011) Surface effects on the postbuckling of nanowires. J Phys D Appl Phys 44(42):425304
26. Bar On B, Altus E (2011) Effects of local surface residual stresses on the near resonance vibrations of nano-beams. J Sound Vib 330(4):652–663
27. Wang G-F, Feng X-Q (2007) Effects of surface elasticity and residual surface tension on the natural frequency of microbeams. Appl Phys Lett 90(23):231904
28. Giunta G, Koutsawa Y, Belouettar S, Hu H (2013) Static, free vibration and stability analysis of three-dimensional nano-beams by atomistic refined models accounting for surface free energy effect. Int J Solids Struct 50(9):1460–1472
29. Zhan H, Gu Y (2012) Surface effects on the dual-mode vibration of$\langle 1\ 1\ 0\rangle$ silver nanowires with different cross-sections. J Phys D Appl Phys 45(46):465304
30. Lei X, Natsuki T, Shi J, Ni Q (2012) Surface effects on the vibrational frequency of double-walled carbon nanotubes using the nonlocal Timoshenko beam model. Compos Part B Eng 43(1):64–69
31. Hosseini-Hashemi S, Fakher M, Nazemnezhad R, Haghighi M-HS (2014) Dynamic behavior of thin and thick cracked nanobeams incorporating surface effects. Compos Part B Eng 61:66–72
32. Hosseini-Hashemi S, Fakher M, Nazemnezhad R (2013) Surface effects on free vibration analysis of nanobeams using nonlocal elasticity: a comparison between Euler–Bernoulli and Timoshenko. J Solid Mech 5(3):290–304
33. Gheshlaghi B, Hasheminejad SM (2012) Vibration analysis of piezoelectric nanowires with surface and small scale effects. Curr Appl Phys 12(4):1096–1099
34. Wang K, Wang B (2012) The electromechanical coupling behavior of piezoelectric nanowires: surface and small-scale effects. Europhys Lett 97(6):66005
35. Yan Z, Jiang L (2011) Electromechanical response of a curved piezoelectric nanobeam with the consideration of surface effects. J Phys D Appl Phys 44(36):365301
36. Yan Z, Jiang L (2011) Surface effects on the electromechanical coupling and bending behaviours of piezoelectric nanowires. J Phys D Appl Phys 44(7):075404
37. Yan Z, Jiang L (2011) The vibrational and buckling behaviors of piezoelectric nanobeams with surface effects. Nanotechnology 22(24):245703
38. Yan Z, Jiang L (2012) Surface effects on the electroelastic responses of a thin piezoelectric plate with nanoscale thickness. J Phys D Appl Phys 45(25):255401
39. Yan Z, Jiang L (2012) Surface effects on the vibration and buckling of piezoelectric nanoplates. Europhys Lett 99(2):27007
40. Zhang J, Wang C, Adhikari S (2012) Surface effect on the buckling of piezoelectric nanofilms. J Phys D Appl Phys 45(28):285301
41. Hosseini-Hashemi S, Nahas I, Fakher M, Nazemnezhad R (2014) Nonlinear free vibration of piezoelectric nanobeams incorporating surface effects. Smart Mater Struct 23(3):035012
42. Hosseini-Hashemi S, Nahas I, Fakher M, Nazemnezhad R (2013) Surface effects on free vibration of piezoelectric functionally graded nanobeams using nonlocal elasticity. Acta Mech. doi:10.1007/s00707-013-1014-z
43. Liu C, Rajapakse R (2010) Continuum models incorporating surface energy for static and dynamic response of nanoscale beams. Nanotechnol IEEE Trans 9(4):422–431
44. Fu Y, Zhang J, Jiang Y (2010) Influences of the surface energies on the nonlinear static and dynamic behaviors of nanobeams. Physica E 42(9):2268–2273
45. Lim C, He L (2004) Size-dependent nonlinear response of thin elastic films with nano-scale thickness. Int J Mech Sci 46(11):1715–1726
46. Nazemnezhad R, Salimi M, Hosseini-Hashemi S, Sharabiani PA (2012) An analytical study on the nonlinear free vibration of nanoscale beams incorporating surface density effects. Compos Part B Eng 43:2893–2897
47. Nayfeh AH, Balachandran B (1989) Modal interactions in dynamical and structural systems. Appl Mech Rev 42(11):175–201
48. Anderson T, Balachandran B, Nayfeh A (1994) Nonlinear resonances in a flexible cantilever beam. J Vib Acoust 116(4):480–484
49. Anderson T, Nayfeh A, Balachandran B (1996) Experimental verification of the importance of the nonlinear curvature in the response of a cantilever beam. J Vib Acoust 118(1):21–27
50. Ouakad HM, Younis MI (2012) Dynamic response of slacked single-walled carbon nanotube resonators. Nonlinear Dyn 67(2):1419–1436
51. Ouakad HM, Younis MI (2011) Natural frequencies and mode shapes of initially curved carbon nanotube resonators under electric excitation. J Sound Vib 330(13):3182–3195
52. Ouakad HM, Younis MI (2010) Nonlinear dynamics of electrically actuated carbon nanotube resonators. J Comput Nonlinear Dyn 5(1):011009
53. Gheshlaghi B, Hasheminejad SM (2011) Surface effects on nonlinear free vibration of nanobeams. Compos Part B Eng 42(4):934–937

54. Malekzadeh P, Shojaee M (2013) Surface and nonlocal effects on the nonlinear free vibration of non-uniform nanobeams. Compos Part B Eng 52:84–92
55. Jia-Hong Z, Min L, Fang G, Qing-Quan L (2012) Influences of surface effects and large deformation on the resonant properties of ultrathin silicon nanocantilevers. Chin Phys B 21(1):016203
56. Hosseini-Hashemi S, Nazemnezhad R (2013) An analytical study on the nonlinear free vibration of functionally graded nanobeams incorporating surface effects. Compos Part B Eng 52:199–206
57. Asgharifard-Sharabiani P, Haeri-Yazdi MR (2013) Nonlinear free vibrations of functionally graded nanobeams with surface effects. Compos Part B Eng 45(1):581–586
58. Hosseini-Hashemi S, Nazemnezhad R, Bedroud M (2014) Surface effects on nonlinear free vibration of functionally graded nanobeams using nonlocal elasticity. Appl Math Model. doi:10.1016/j.apm.2013.11.068
59. Gheshlaghi B, Hasheminejad SM (2011) Surface effects on nonlinear free vibration of nanobeams. Compos Part B Eng 42(4):934–937
60. Gurtin ME, Ian Murdoch A (1978) Surface stress in solids. Int J Solids Struct 14(6):431–440
61. Chen T, Chiu M-S, Weng C-N (2006) Derivation of the generalized Young–Laplace equation of curved interfaces in nanoscaled solids. J Appl Phys 100(7):074308
62. Rao SS (2007) Vibration of continuous systems. Wiley, New York
63. Azrar L, Benamar R, White R (1999) Semi-analytical approach to the non-linear dynamic response problem of S–S and C–C beams at large vibration amplitudes part I: general theory and application to the single mode approach to free and forced vibration analysis. J Sound Vib 224(2):183–207
64. Azrar L, Benamar R, White R (2002) A semi-analytical approach to the non-linear dynamic response problem of beams at large vibration amplitudes, part II: multimode approach to the steady state forced periodic response. J Sound Vib 255(1):1–41
65. Ke L–L, Yang J, Kitipornchai S (2010) An analytical study on the nonlinear vibration of functionally graded beams. Meccanica 45(6):743–752
66. Chandra R, Raju BB (1975) Large deflection vibration of angle ply laminated plates. J Sound Vib 40(3):393–408
67. Nayfeh AH, Mook DT (2008) Nonlinear oscillations. Wiley, New York
68. Ogata S, Li J, Yip S (2002) Ideal pure shear strength of aluminum and copper. Science 298(5594):807–811
69. Miller RE, Shenoy VB (2000) Size-dependent elastic properties of nanosized structural elements. Nanotechnology 11(3):139
70. Cowper G (1966) The shear coefficient in Timoshenko's beam theory. J Appl Mech 33(2):335–340